JOURNAL OF CATALYSIS 155, 141–147 (1995)

Reaction Mechanisms of Isomerization and Cracking of Heptane on Pd/H-Beta Zeolite

E. Blomsma, J. A. Martens, and P. A. Jacobs

Centrum voor Oppervlaktechemie en Katalyse, Katholieke Universiteit Leuven, Kardinaal Mercierlaan 92, B-3001 Leuven (Heverlee), Belgium

Received December 27, 1994; revised April 11, 1995

The vapor-phase isomerization and cracking of heptane on H-Beta zeolites loaded with various amounts of Pd metal has been studied at a temperature of 505 K and at a total pressure of 0.3 MPa. The cracking of heptane is interpreted as a combination of classic bifunctional hydrocracking and dimerization cracking. The isomerization of heptane proceeds through the classic bifunctional mechanism and a second mechanism involving dimerization cracking. The contribution of the different mechanisms to the isomerization and cracking is derived from the formation of specific reaction products. The contribution of the different mechanisms is dependent on the Pd content of the zeolite.

INTRODUCTION

Bifunctional catalysts combining hydrogenation–dehydrogenation and Brønsted acid functions are widely used in processes of isomerization and hydrocracking of petroleum fractions (1). In typical catalyst formulations, the noble metal catalyzes hydrogenation–dehydrogenation reactions, and the zeolite hydroxyl groups catalyze the carbocation rearrangements. Such catalysts are particularly useful for the branching isomerization of *n*-alkanes with the purpose of enhancing the octane number of automotive fuels. In contrast to monofunctional catalysis, a synergism exists between the two sets of sites in bifunctional catalysts leading to an enhanced catalytic activity, suppressed deactivation, and higher yields of products with tertiary and quaternary C atoms (2). In classic bifunctional isomerization (3), the alkane is first dehydrogenated on the noble metal into an alkene. The alkene migrates to a Brønsted acid site, where it adsorbs to yield an alkylcarbenium ion. The alkylcarbenium ion undergoes skeletal rearrangements, desorbs as an iso-alkene, and migrates to a metal site where it is hydrogenated into the final iso-alkane reaction product. Classic hydrocracking takes place when branched secondary and tertiary alkylcarbenium ions derived from the feed molecule are cleaved by a single β-scission into smaller alkylcarbenium ions and alkenes (4, 5). During hydrocracking, the formation of primary alkylcarbenium ions is unlikely and the carbon number of the fragments from a C_nH_{2n+2} alkane are within the range 3 to n-3 (6). The classic reaction model assumes efficient transport between the metal and acid sites. The average spatial separation of the two types of catalytic sites can be estimated using the Weisz criterion (7). The distribution of metal and acid sites on the catalyst surface not only influences the catalytic activity but has a strong influence on product selectivity as well.

Different situations have been identified by Giannetto and co-workers in the conversion of heptane on H–Y, H–MOR (8), and H–ZSM-5 zeolites loaded with platinum metal (8, 9), based on the number of strong acid sites characterized by a heat of adsorption of ammonia exceeding 100 kJ/mol. When the ratio of strong acid sites to metal sites on H–Y or H–ZSM-5 zeolite exceeds a value of 33, acid catalysis predominates since alkenes are hydrogenated on a metal site only after multiple conversions on acid sites. In this case all types of reaction products, viz. mono- and multibranched isoheptanes as well as cracked products, appear as primary reaction products. On catalysts with strong acidity, olefinic reaction intermediates may dimerize, rapidly crack, and generate cracked products which cannot be formed via classic hydrocracking (10–13). In this way, from a C_7 feed, C_5 and C_6 fragments are obtained. When the ratio of strong acid sites to metal sites is below 6, a Pt/H–Y catalyst shows optimum performance with respect to isomerization (8). In the case of a heptane feed, monobranched and dibranched isoheptanes and cracked products are formed consecutively. Similar changes in the reaction network depending on the balance of hydrogenating and acid functions have been reported by Degnan and Kennedy (14), who studied heptane isomerization and cracking on physical mixtures of Pt/Al_2O_3 particles and zeolite H-Beta crystals with a Si/Al ratio of 68. An acid–metal balance for this Pt/Al_2O_3 and zeolite H-Beta mixture is achieved when one surface

0021-9517/95 $12.00

Pt atom is present for every six framework aluminum atoms. Since each Al atom in the framework of zeolite H-Beta is associated with a strong Brønsted acid site, the critical acid to metal ratio for zeolite H-Beta is the same as for Pt/H-Y zeolite (8).

In this work we studied the conversion of heptane on commercial zeolite H-Beta crystals with a Si/Al ratio of 12.5, on which the noble metal was supported. Because of its low hydrogenolysis activity compared to platinum, Pd metal was selected for its hydrogenation–dehydrogenation function (15). Palladium has a weaker hydrogenation–dehydrogenation activity compared to platinum (16). It was found that the conversion of heptane on Pd/H-Beta catalysts cannot be rationalized solely based on the classic bifunctional reaction scheme. Depending on the Pd loading, additional mechanisms of dimerization cracking have to be invoked to explain the observed product patterns.

EXPERIMENTAL

According to the manufacturer (PQ Corporation, Sample 304, CBV811-25), the Si/Al ratio, specific surface area, and crystal size of the H-Beta zeolite sample were 12.5, 750 m^2/g, and 0.1–0.7 μm, respectively. Palladium was deposited on the zeolite by incipient wetness impregnation of an aqueous solution of the tetramine-dichloride salt.

Heptane conversion was carried out in a fully automated continuous flow tubular microreactor. 500 mg of catalyst was activated *in situ* in the reactor by calcination in flowing oxygen (15 mol kg^{-1} s^{-1}) at 400°C, followed by reduction in hydrogen under the same conditions. A stream of hydrogen saturated with heptane vapour was generated using a thermostatted saturator. The purity of heptane was at least 99%, the main impurities being isomers of heptane. The reaction products were analyzed online with a HP5890II gaschromatograph, equipped with a 50 m CPSil5 column (Chrompack) and an FID or MSD detector. All reaction products were identified as alkanes.

The yield of a cracked product fraction with carbon number i, $Y^*_{C_i}$, is calculated as follows:

$$Y^*_{C_i} = \left(\frac{1}{i}\sum_{j=1}^{n_j} A_{i,j} \Big/ \frac{1}{7}\sum_{i=1}^{6}\sum_{j=1}^{n_j} A_{i,j}\right) \times 100.$$

$A_{i,j}$ represents the peak area in the chromatogram of reaction product j with carbon number i, and n_j represents the number of products with carbon number j. The yield of cracked products $Y^*_{C_i}$ is expressed as mol per 100 mol of cracked heptane.

The yield of isomerization Y_{iso} (%), is calculated in the conventional way, considering $A_{7,1}$ as the peak area of heptane,

$$Y_{iso} = \left(\sum_{j=2}^{n_7} A_{7,j} \Big/ \sum_{i=1}^{7}\sum_{j=1}^{n_j} A_{i,j}\right) \times 100.$$

In most experiments, the space time (W/F_0, in which W is the amount of catalyst and F_0 the molar flow rate of heptane at the reactor entrance) was adjusted to reach 82.5% conversion of heptane. The actual reaction temperature was 505 K, the hydrogen/heptane molar ratio was 60, and the total pressure was 0.3 MPa. Under these conditions, the reaction products are a mixture of cracked products (having a carbon number smaller than 7) and isomerization products (having a branched carbon skeleton and a carbon number of 7). Cracking and isomerization reactions are discussed separately.

RESULTS AND DISCUSSION

Classic Hydrocracking versus Dimerization Cracking

The yield of the different cracked product fractions obtained on Pd/H-Beta catalysts with different Pd contents is given in Table 1. For Pd loadings between 0.1 and 1.5 wt%, C_4 cracked products are formed in excess of C_3 products, C_5 and C_6 products are formed in small quantities, while C_1 and C_2 products are absent. The absence of methane and ethane reveals that hydrogenolysis does not contribute to the cracking (16).

Classic hydrocracking of heptane exclusively results in the formation of equimolar amounts of C_3 and C_4 products adding up exactly to 200 mol products formed per 100 mol of feed cracked (17). Since less than 200 mol of cracked products are formed on the Pd/H-Beta zeolites tested, other cracking mechanisms besides classic hydrocracking

TABLE 1

Heptane Conversion on Pd/H-Beta Catalysts[a]

wt% Pd	0.10	0.25	1.00	1.50
Y_{iso} (%)	56.4	66.0	73.2	73.2
Activity[b] (mol h^{-1} kg^{-1})	9	18	25	30
Y^*_{C3} (mol/100 mol)	94.1	95.8	95.2	98.4
Y^*_{C4} (mol/100 mol)	103.0	100.9	100.4	100.6
Y^*_{C5} (mol/100 mol)	0.4	0.5	0.6	0.3
Y^*_{C6} (mol/100 mol)	0.6	1.1	1.7	0.3
$\sum_{i=1}^{6} Y^*_{Ci}$ (mol/100 mol)	198.1	198.3	197.9	199.6
i/nC_4	119	75	83	89
i/nC_5	2.4	1.6	—	—
i/nC_6	1.7	1.6	1.4	—
DC (%)	5	3.4	3.8	1.4
HC (%)	95.0	96.6	96.2	98.6

[a] $Y^*_{C1} = Y^*_{C2} = 0.0$ mol/100 mol.

[b] The activity is obtained by $A = 100 \times$ (conversion)/(space time).

should be involved. The formation of C_5 and C_6 products cannot originate from β-scission of C_7 alkylcarbenium ions, since methane and ethane abstraction are unfavourable (18), but should stem from β-scissions of heavier alkylcarbenium ions. A likely reaction pathway explaining their formation involves the dimerization of heptenes followed by recracking of the C_{14} molecule. This type of cracking corresponds to the dimerization cracking (DC) reactions previously suggested (10, 19–22).

The following approach was used to estimate the contribution of dimerization cracking (DC) and classic hydrocracking (HC). The contribution of classic hydrocracking is estimated as the molar yield of C_3 and an equimolar yield of C_4. Scissions not resulting in 1 C_3 and 1 C_4 fragments are ascribed to dimerization cracking. Thus, the contribution of dimerization cracking is estimated as the excess molar yield of C_4 with respect to C_3 and the molar yield of C_5 and C_6 products. The contribution of dimerization cracking and classic hydrocracking with respect to total C_7 cracking are obtained from

$$DC = 100(Y^*_{(C4+C5+C6)} - Y^*_{C3})/\sum_{i=1}^{6} Y^*_{Ci} \quad (\% \text{ of total } C_7 \text{ cracking})$$

$$HC = 100(2Y^*_{C3})/\sum_{i=1}^{6} Y^*_{Ci} \quad (\% \text{ of total } C_7 \text{ cracking}).$$

It has to be stressed that calculated DC and HC values represent only an estimation of the contribution of these cracking mechanisms, useful in a discussion of the impact of catalyst properties. In the approach followed, C_3 fragments from dimerization cracking can not be discriminated from products from classic hydrocracking and are counted as classic hydrocracking products. The DC and HC values for the series of Pd/H-Beta zeolites investigated are reported in Table 1. Dimerization cracking reactions are most important at low metal loadings (0.10 wt% Pd). Under conditions of dimerization cracking, the total yield of cracked products drops below 200 mol per 100 mol of heptane cracked. Indeed, in dimerization cracking, less than two fragments are obtained per C_7 molecule cracked. A typical conversion is, e.g., the cracking of 2 C_7 molecules into 1 C_4 and 2C_5 fragments.

Dimerization Cracking Reaction Pathways

In the conversion of heptane on Pt/H-ZSM-5- and Pt/H-Y-type catalysts, dimerization cracking has been described as a fast dimerization of heptane followed by isomerization and fragmentation of the C_{14} intermediate (23, 24). The product distributions obtained from dimerization cracking of heptane have been explained based on the reaction shown in Scheme 1 (8, 10, 11):

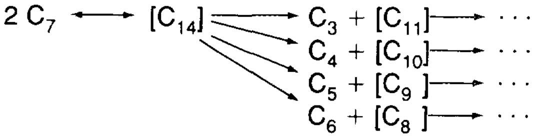

$$2\,C_7 \longleftrightarrow [C_{14}] \rightarrow \begin{cases} C_3 + [C_{11}] \rightarrow \cdots \\ C_4 + [C_{10}] \rightarrow \cdots \\ C_5 + [C_9\,] \rightarrow \cdots \\ C_6 + [C_8\,] \rightarrow \cdots \end{cases}$$

SCHEME 1

The reactivity of alkanes towards cracking increases with the carbon number (5). Under a reaction severity at which C_7 cracks, the fragments from dimerization cracking with a carbon number exceeding 7 crack more rapidly and are not observed as reaction products. In Scheme 2, proposed by López Agudo *et al.* for heptane cracking on a CrHNaY catalyst, the cracking does not yield fragments larger than C_7 (10):

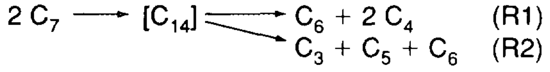

$$2\,C_7 \rightarrow [C_{14}] \rightarrow \begin{cases} C_6 + 2\,C_4 & (R1) \\ C_3 + C_5 + C_6 & (R2) \end{cases}$$

SCHEME 2

The formation of pentane can arise from reaction R2 only. Therefore, it is possible to calculate the contributions of reactions R1 and R2 in dimerization cracking based on experimentally obtained cracked product yields. An attempt to explain the product distribution from heptane cracking on 1.0 wt% Pd/H-Beta according to the dimerization cracking reactions of scheme 2 is developed in Table 2.

The occurrence of reactions R1 and R2 explains the presence of C_5 and C_6, but cannot account for the excess of C_4 compared to C_3. If R2 is replaced by an alternative reaction path (R3 in Scheme 3) in which the C_{14} intermediate cracks into one C_4 and two C_5 fragments,

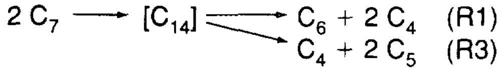

$$2\,C_7 \rightarrow [C_{14}] \rightarrow \begin{cases} C_6 + 2\,C_4 & (R1) \\ C_4 + 2\,C_5 & (R3) \end{cases}$$

SCHEME 3

a better agreement of C_3 and C_4 yields is obtained (Table 3). In principle, the C_3 and C_4 yields should be identical

TABLE 2

Cracking of Heptane on 1.0 wt% Pd/H-Beta

	C_3	C_4	C_5	C_6
Y^*_{Ci}, exp	95.2	100.4	0.6	1.7
Y^*_{Ci}, DC_{R1}	—	2.2	—	1.1
Y^*_{Ci}, DC_{R2}	0.6	—	0.6	0.6
Y^*_{Ci}, exp-Y^*_{Ci}, DC_{R1}− Y^*_{Ci}, DC_{R2}	94.6	98.2	0	0

Note. The attempt to rationalize cracking is based on hydrocracking and dimerization cracking according to Scheme 2. exp = experimental results; DC_{Ri} = dimerization cracking reaction R*i*.

TABLE 3

Cracking of Heptane on 1.0 wt% Pd/H-Beta

	C_3	C_4	C_5	C_6
Y^*_{Ci}, exp	95.2	100.4	0.6	1.7
Y^*_{Ci}, DC_{R1}	—	3.4	—	1.7
Y^*_{Ci}, DC_{R3}	—	0.3	0.6	—
Y^*_{Ci}, exp-Y^*_{Ci}, DC_{R1} − Y^*_{Ci}, DC_{R3}	95.2	96.7	0	0

Note. The attempt to rationalize cracking is based on hydrocracking and dimerization-cracking according to Scheme 3. exp = experimental results; DC_{Ri} = dimerization cracking reaction Ri.

after substraction of the yields from dimerization cracking. The remaining imbalance in the distribution can be ascribed to reactions between heptenes and olefinic cracking products (24, 25).

The low contribution of R2 with respect to R1 and R3 is in agreement with the cracking behaviour of long-chain *n*-alkanes on Pt/H-Beta zeolites, for which propane abstractions are much slower than C–C bond scissions closer to the center of the chain (17, 26, 27).

Conversion patterns of *n*-alkanes on Pt/H-Beta are available from the literature (26, 27). In the conversion of long-chain alkanes such as *n*-C_{14}, hydrocracking is preceeded by isomerization. The cracked product yields from the cracking of *n*-C_{14} with secondary cracking of all primary fragments larger than C_7 are given in Table 4. In the simulation in Table 4, it is assumed that the large primary fragments are cracked according to the cracking modes of the corresponding *n*-alkanes, available from the literature.

The yield of fragments decreases in the order $C_4 > C_5 > C_6$. In dimerization cracking, the product yields obey a different order, $C_4 \gg C_6 \geq C_5$ (Tables 1–3). Moreover, in hydrocracking of *n*-C_{14} the ratio of branched to linear fragments in the C_5 and C_6 fractions is much higher (i/n = 7, Table 4) than that in dimerization cracking (i/n = 1.4 to 2.4, Table 1). It is concluded that the cracking modes of the C_{14} intermediate in C_7 dimerization cracking and of isomerized tetradecanes are different.

An example of dimerization of two heptane molecules into a C_{14} intermediate and the subsequent cracking, without skeletal isomerization of the intermediate, is depicted in Fig. 1. In the example shown, an addition of a hept-2-yl cation on a hept-2-ene molecule takes place. In the C_{14} alkylcarbenium ion obtained, the positive charge can be shifted along the carbon skeleton via hydride shifts to yield an isomer which is subsceptible to β-scission reactions not leading to primary cations. Neither methyl shifts nor branching isomerization steps need to be involved. Hydride shifts are not always required in order to reach a C_{14} alkylcarbenium ion intermediate that is susceptible to β-scission. An example of *direct* dimerization cracking is given in Fig. 2.

Table 5 summarizes the possible dimerization cracking pathways of heptane. Most of the additions of unbranched or monobranched C_7 cations on unbranched or monobranched C_7 alkenes yield C_{14} cations that are susceptible to β-scission, after having undergone the necessary hydride shifts. The reaction pathways developed in Table 5

TABLE 4

Yield of Cracked Product Fractions from Cracking of 100 mol of *n*-C_{14} on Pt/H-Beta Zeolite Assuming Recracking of the Primary C_8-C_{11} Fragments According to the Patterns for the Corresponding *n*-alkanes (Data from Refs. (17, 25, 26))

CN	3	4	5	6	7	8	9	10	11	14
Y^*	4	28	28	28	24	28	28	28	4	CR
	0	2	2	2	2				CR	
	2	16	20	16	2			CR		
	5	23	23	5			CR			
	11	33	11			CR				
Y^*	22	102	84	51						
i/n			7	7						

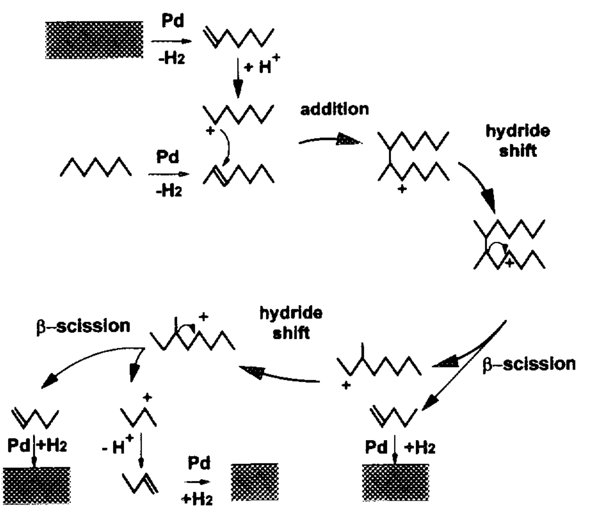

FIG. 1. Example of a dimerization cracking pathway involving alkene-alkylcarbenium ion addition, hydride shifts, and β-scissions.

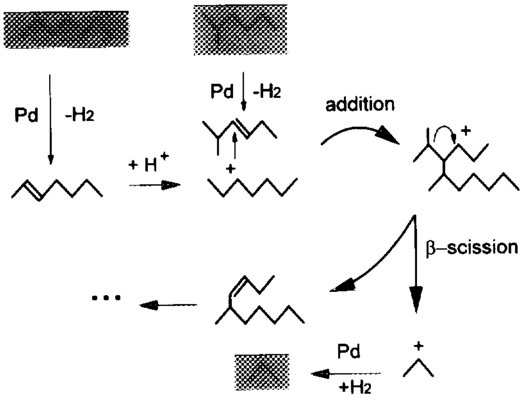

FIG. 2. Example of a direct dimerization cracking pathway involving alkene-alkylcarbenium ion addition and β-scissions.

TABLE 5

Reaction Products from Selected Dimerization-Cracking Reactions of Heptane and its Isomers on Bifunctional Catalysts Involving Alkylcarbenium Ion–Alkene Addition, Hydride Shifts, and β-Scissions

	$2Me2C_6^+$	$3Me3C_6^+$	$2C_7^+$	$3C_7^+$	$4C_7^+$
$1C_7^=$	—[a]	—	—	—	—
$2C_7^=$	$n_4 + n_5 + i_5$	$n_3 + n_5 + i_6$	$n_4 + 2n_5$	$n_4 + 2n_5$	$n_3 + n_5 + n_6$
$3C_7^=$	$2n_4 + i_6$	—	$n_4 + 2n_5$	$2n_4 + n_6$	—
$2Me1C_6^=$	$2n_4 + i_6$	—	$n_4 + n_5 + i_5$	$2n_4 + i_6$	—
$2Me2C_6^=$	$3n_3 + n_5$ $n_4 + n_5 + i_5$ $2n_4 + i_6$	$3n_3 + i_5$	$3n_3 + n_5$ $n_3 + n_5 + n_6$ $n_4 + n_5 + i_5$	$2n_4 + i_6$	$3n_3 + n_5$
$2Me3C_6^=$	$n_4 + i_4 + i_6$	$3n_3 + i_5$	$3n_3 + n_5$ $n_3 + n_5 + i_6$ $n_3 + n_5 + n_6$ $i_4 + n_5 + i_5$	$n_4 + i_4 + i_6$	$3n_3 + n_5$
$2Me4C_6^=$	$n_3 + n_5 + i_6$ $n_4 + i_4 + i_6$	$n_3 + i_5 + i_6$	$n_3 + n_5 + i_6$ $n_4 + n_5 + i_5$ $i_4 + 2n_5$	$n_4 + n_5 + i_5$ $n_4 + i_4 + n_6$	$n_3 + i_5 + n_6$
$2Me5C_6^=$	$n_3 + n_5 + i_6$	$n_3 + i_5 + i_6$	$n_3 + n_5 + i_6$ $n_3 + n_5 + n_6$ $n_4 + n_5 + i_5$	$n_4 + n_5 + i_5$	$n_3 + i_5 + n_6$
$3Me1C_6^=$	$n_4 + n_5 + i_5$	$n_3 + n_5 + i_6$	$n_3 + n_5 + n_6$ $n_4 + 2n_5$	$n_4 + 2n_5$	$n_3 + n_5 + n_6$
$3Me2C_6^=$	$n_4 + n_5 + i_5$	$n_3 + n_5 + i_6$	$n_3 + n_5 + i_6$ $n_4 + 2n_5$	$n_4 + 2n_5$	$n_3 + n_5 + n_6$
$3Me3C_6^=$	$2n_4 + i_6$	—	$n_3 + n_5 + i_6$ $n_4 + 2n_5$	$2n_4 + n_6$	—
$3Me4C_6^=$	$2n_4 + i_6$ $n_4 + 2i_5$	$n_3 + i_5 + i_6$	$n_4 + n_5 + i_5$ $n_4 + 2n_5$	$n_4 + n_5 + i_5$ $2n_4 + n_6$	$n_3 + i_5 + i_6$
$3Me5C_6^=$	$n_4 + 2i_5$	$n_3 + i_5 + i_6$	$n_4 + n_5 + i_5$ $n_4 + 2n_5$	$n_4 + n_5 + i_5$ $2n_4 + n_6$	$n_3 + i_5 + i_6$

Note: Carbocations and olefins are given as $yC_7^{+(=)}$ or x Me y $C_6^{+(=)}$, in which x gives the location of the methylbranching and y the location of the positive charge or double bond, respectively. i_z stands for the branched and n_z for the linear fragments with carbon number z.

[a] Dimerization cracking requires an alkyl shift on the C_{14} intermediate.

allow one to conclude that dimerization cracking reactions can yield all individual linear and branched C_3–C_6 reaction products observed experimentally. However, dimerization cracking via additions of branched heptyl cations to branched or unbranched heptenes are expected to be dominant over additions of *n*-heptyl cations (20). The nature of the cracked products depends on the degree of branching of the C_{14} intermediate. In dimerization cracking, linear fragments are abundantly formed (Tables 1 and 5). The reason for this is that skeletal branching isomerization of the C_{14} intermediate does not occur before β-scission, and that branched C_7 molecules apparently show less tendency to dimerize. The suppression of this type of reaction is ascribed to a molecular shape-selective effect of H-Beta zeolite.

Isomerization via Dimerization Cracking

Besides C_3–C_6 products, branched C_7 molecules can be generated by dimerization cracking reactions as well. Thus on catalysts favouring dimerization cracking (low Pd content), branched C_7 isomers can be expected to be generated through dimerization cracking as well as through classic bifunctional isomerization. Some specific C_7 isomers can only be generated through the classic bifunctional isomerization. These are 3-ethylpentane, 2, 2- and 3,3-dimethylpentane, and 2,2,3-trimethylbutane. β-scission yields exclusively methylbranched fragments (17), and for this reason, 3-ethylpentane cannot be formed through dimerization cracking. It has been demonstrated that hydrocracking of long-chain *n*-alkanes via β-scission of branched alkylcarbenium ions cannot lead to the formation of fragments with a quaternary carbon atom (28, 29). Classic branching isomerization of heptane can generate molecules with ethylbranching and molecules with quaternary carbon atoms (4).

Discrimination among the two mechanisms is possible based on the formation of these specific isomers. The mono- and dibranched C_7 molecules that can be generated from dimerization of two C_7 molecules followed by β-scission of the C_{14} intermediate are 2-methylhexane, 3-methylhexane, 2,3-dimethylpentane, and 2,4-dimethylpentane. The formation of 3-ethylpentane, 2,2-dimethylpentane, and 3,3-dimethylpentane products is expected to be suppressed when dimerization cracking is important, since they must originate from classic bifunctional isomerization reactions.

TABLE 6

Distribution and Yield of the Monobranched C_7 Isomers (%) in the Conversion of Heptane on Pd/H-Beta

wt% Pd	0.10	0.25	1.00	1.50
$2MeC_6$	49.7	49.2	48.8	48.5
$3MeC_6$	48.0	47.8	47.8	47.9
$3EtC_5$	2.2	2.9	3.5	3.6
Y^{iso}_{mono} (%)	43.3	49.4	52.3	53.1

TABLE 7

Distribution and Yield of the Multibranched C7 Isomers (%) in the Conversion of Heptane on Pd/H-Beta

wt% Pd	0.10	0.25	1.00	1.50
$2{,}2diMeC_5$	17	21	28	26
$2{,}3diMeC_5$	39	36	31	32
$2{,}4diMeC_5$	39	34	28	29
$3{,}3diMeC_5$	5	7	12	11
$2{,}2{,}3triMeC_4$	1	2	2	2
Y^{iso}_{multi} (%)	13.1	16.6	20.9	20.2

The distribution of mono- and dibranched isoheptanes obtained on Pd/H-Beta zeolites with increasing Pd content is given in Tables 6 and 7, respectively. At low Pd loading, where the contribution of the DC mechanism is most important, the formation of isomers with a quaternary C atom is disfavoured, indeed, as is the formation of 3-ethylpentane. In the literature it is reported that on the solid superacid catalyst Pt/ZrO_2–SO_4, the shift towards C_4–C_6 cracked products and the suppressed formation of 2,2-dimethyl-, 3,3-dimethyl-, and 3-ethylpentane is even more pronounced (30).

Catalyst Pd Content and the Contribution of Cracking Mechanisms

In Fig. 3, a qualitative picture of the contribution of the different cracking mechanisms operative in heptane conversion on Pd/H-Beta catalysts is presented. Dimerization cracking, although less important than classic hydrocracking, is active even at a high Pd loading of 1.5 wt%. For these catalysts, the heptane conversion rate follows a negative-order dependence in hydrogen, thus

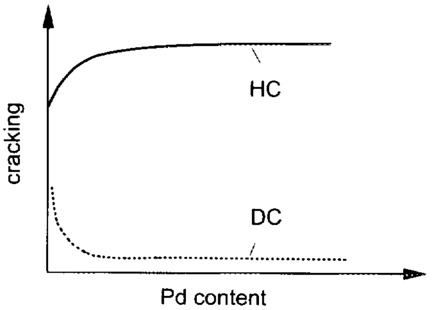

FIG. 3. Evaluation of the contribution of classic hydrocracking (HC) and dimerization cracking (DC) to cracking with the Pd content of Pd/H-Beta.

confirming the bifunctional mechanism (31). On 0.25 wt% Pd/H-Beta as well as on 1.00 wt% Pd/H-Beta, an apparent hydrogen order of −0.5 was measured.

CONCLUSION

The classic bifunctional mechanism for isomerization and hydrocracking does not offer an explanation for the detailed features of heptane conversion on Pd/H-Beta zeolite catalysts. On these zeolites, additional isomerization and cracking mechanisms are operative, involving addition reactions of C_7 alkenes and C_7 alkylcarbenium ions. In dimerization cracking, a C_{14} alkylcarbenium ion is cracked via β-scission into C_3–C_6 fragments. The nature of these C_{14} intermediates and their cracking modes are different from the C_{14} species that occur as intermediates in the hydrocracking of n-C_{14}. The dimerization cracking mechanism has been suggested in previous studies on heptane hydrocracking in bifunctional zeolites (8, 10, 11). In the present work, the fastest dimerization cracking reaction pathways not involving skeletal rearrangements of the C_{14} intermediates are identified. C_7 isomerization through dimerization and cracking occurs under conditions where dimerization cracking is operative. The dimerization cracking mechanism is active even at a Pd loading as high as 1.5 wt%.

ACKNOWLEDGMENTS

This is part of the Ph.D. work of E. B., sponsored by Shell Research B.V. J.A.M. acknowledges the Flemish NFWO for a Research Position as Senior Research Associate. A research grant from the Belgian government within the frame of the IUAP is highly appreciated.

REFERENCES

1. Maxwell, I. E., and Stork, W. H. J., *Stud. Surf. Sci. Catal.* **58,** 571 (1991).
2. Pichler, H., Shultz, H., Reitemeyer, H. O., and Weitkamp, J., *Erdöl Kohle. Erdgas. Petrochem.* **25,** 494 (1982).
3. Coonradt, M. L., and Garwood, W. E., *Ind. Eng. Chem. Prod. Res. Dev.* **3,** 38 (1964).
4. Weitkamp, J., *Erdöl Kohle. Erdgas. Petrochem.* **31,** 13 (1978).
5. Weitkamp, J., *in* "Hydrocracking and Hydrotreating," (J. W. Waid and G. A. Quader, Eds.), ACS Symp. Ser. Vol. **20,** p. 1. Am. Chem. Soc., Washington, DC (1975).
6. Weitkamp, J., Jacobs, P. A. and Martens, J. A., *Appl. Catal.* **8,** 123 (1983).
7. Weisz, P. B., *Adv. Catal.* **13,** 137 (1962).
8. Guisnet, M., Alvarez, F., Giannetto, G., and Perot, G., *Catal. Today* **1,** 415 (1987).
9. Alvarez, F., Ribeiro, F. R., Giannetto, G., Chevalier, F., Perot, G., and Guisnet, M., *Stud. Surf. Sci. Catal.* **46,** 1339 (1989).
10. Lopéz Agudo, A., Asensio, A., and Corma, A., *J. Catal.* **69,** 274 (1981).
11. Giannetto, G., Perot, G., and Guisnet, M., *in* "Catalysis by Acids and Bases," p. 265. Elsevier, Amsterdam/New York (1984).
12. Smirniotis, P. G., and Ruckenstein, E., *J. Catal.* **140,** 526 (1993).
13. Leglise, J., Chambellan, A., and Cornet, D., *Appl. Catal.* **69,** 15 (1991).
14. Degnan, T. F., and Kennedy, C. R., *AIChE J.* **39**(4), 607 (1993).
15. Clarke, J. K. A., and Rooney, J. J., *Adv. Catal.* **25,** 125 (1976).
16. Carter, J. L., Cusumano, J. A., and Sinfelt, J. H., *J. Catal.* **20,** 223 (1971).
17. Martens, J. A., Jacobs, P. A., and Weitkamp, J., *Appl. Catal.* **20,** 239 (1986).
18. Brouwer, D. M., *NATO Avd. Stud. Inst. Ser. E* (Prins, R., and Schuit, G. C. A., Eds.), **39,** 137 (1980).
19. Dejaifve, P., Véndrine, J. C., Bolis, V., and Derouane, E. G., *J. Catal.* **63,** 331 (1980).
20. Abbot, J., and Wojciechowski, B. W., *Can. J. Chem. Eng.* **63,** 278, 451, 462 (1985).
21. Abbot, J., Corma, A., and Wojciechowski, B. W., *J. Catal.* **92,** 398 (1985).
22. Dooley, K. M., and Gates, B. C., *J. Catal.* **96,** 347 (1985).
23. Fuentes, G. A., and Gates, B. C., *J. Catal.* **76,** 440 (1982).
24. Lin, L., Gnep, N. S., and Guisnet, M. R., *in* Symposium on the Hydrocarbon Chemistry of FCC Naphta Formation, Div. Petr. Chem., Miami Meeting," p. 687. Am. Chem. Soc., New York (1989).
25. Zainuddin, Z., Guerzoni, F. N., and Abbot, J., *J. Catal.* **140,** 150 (1993).
26. Martens, J. A., Tielen, M., and Jacobs, P. A., *Catal. Today* **1,** 435 (1987).
27. Martens, J. A., Perez-Pariente, J., and Jacobs, P. A., "Proceedings International Symposium on Zeolite Catalysis," Siofok, Hungary, 1985, p. 487.
28. Martens, J. A., Jacobs, P. A., and Weitkamp, J., *Appl. Catal.* **20,** 283 (1986).
29. Schultz, H., and Weitkamp, J., *Prepr. Div. Petr. Chem. Am. Chem. Soc.* **17**(4), 84 (1972).
30. Iglesia, E., Soled, S. L., and Kramer, G. M., *J. Catal.* **144,** 238 (1993).
31. Belloum, M., Tavers, Ch., and Bournonville, J. P., *Rev. Inst. Fr. Pét.* **46**(1), 89, 1991.